The Astrophysical Journal, 639:L91–L94, 2006 March 10

SUPERDIFFUSIVE AND SUBDIFFUSIVE TRANSPORT OF ENERGETIC PARTICLES IN SOLAR WIND ANISOTROPIC MAGNETIC TURBULENCE

G. Zimbardo, P. Pommois, and P. Veltri
Physics Department, University of Calabria, Arcavacata di Rende, 87036 Rende, Italy; zimbardo@fis.unical.it, pommois@fis.unical.it, veltri@fis.unical.it
Received 2005 June 6; accepted 2006 January 26; published 2006 February 13

ABSTRACT

The transport of energetic particles in a mean magnetic field and the presence of anisotropic magnetic turbulence are studied numerically, for parameter values relevant to the solar wind. A numerical realization of magnetic turbulence is set up in which we can vary the type of anisotropy by changing the correlation lengths l_x, l_y, l_z. We find that for l_x, $l_y \gg l_z$, transport can be non-Gaussian, with superdiffusion along the average magnetic field and subdiffusion perpendicular to it. Decreasing the l_x/l_z ratio down to $\lesssim 0.3$, Gaussian diffusion is obtained, showing that the transport regime depends on the turbulence anisotropy. Implications for energetic particle propagation in the solar wind and for diffusive shock acceleration are discussed.

Subject headings: diffusion — plasmas — solar wind — turbulence

1. INTRODUCTION

Many studies have addressed the transport of energetic particles in the heliosphere in the presence of magnetic turbulence, both from the theoretical (Jokipii 1966; Jokipii & Parker 1969; Giacalone & Jokipii 1999; Teufel & Schlickeiser 2002; Matthaeus et al. 2003; Shalchi et al. 2004) and from the observational point of view (Reames 1999; Mazur et al. 2000; Dalla et al. 2003; Zhang et al. 2003; McKibben 2005), but a full understanding is still lacking. For instance, the computed values of the perpendicular diffusion coefficient $\kappa_\perp$ are 1–2 orders of magnitude smaller than those inferred from the observations of solar energetic particles (SEPs) at widely separated spacecraft (Ruffolo et al. 2003; McKibben 2005). On the other hand, large values of $\kappa_\perp$ are in seeming contrast to the observations of particle dropouts in the 10 keV–1 MeV particle fluxes in impulsive SEP events (Mazur et al. 2000) and with the finding of sharp composition boundaries in *Ulysses* data (Zurbuchen et al. 2000), which indicate a small cross-field transport. Also, a parallel mean free path $\lambda_\parallel$ of the order of 0.1–0.2 AU is often assumed for 10 MeV protons (Bieber et al. 1994), but the time of arrival of solar particles at 1 AU has often been found to be consistent with scatter-free propagation (Reames 1999; Dalla et al. 2003; Zhang et al. 2003), corresponding to $\lambda_\parallel \sim 1$ AU or more.

These puzzling observational data call for new ideas and new theoretical tools, like anomalous transport (Zimbardo & Veltri 1995), non-Markovian phenomena (Kóta & Jokipii 2000; Qin et al. 2002a), different transport regimes inside and in between coherent magnetic flux tubes (Ruffolo et al. 2003), and the non-Gaussian nature of turbulent transport (Zimbardo et al. 2004), in order to be able to reconcile theory and observations. As a step in this direction, here we explore numerically the influence of turbulence anisotropy on transport regimes. Solar wind magnetic turbulence is known to be anisotropic (Dobrowolny et al. 1980; Matthaeus et al. 1996), but the kind of anisotropy is not easily determined by single spacecraft observations. Turbulence models range from one-dimensional, or slab (Jokipii 1966; Teufel & Schlickeiser 2002), with the wavevectors aligned along the background magnetic field $\boldsymbol{B}_0$, to two-dimensional (Bieber et al. 1996), with the wavevectors perpendicular to $\boldsymbol{B}_0$, to fully three-dimensional (Carbone et al. 1995; Matthaeus et al. 1996). Knowledge of the spectral distribution of magnetic fluctuations in $\boldsymbol{k}$-space is fundamental to foresee the effect of magnetic turbulence on particle transport; indeed, wave-particle interactions sensitively depend on the wavevector distribution.

2. NUMERICAL STUDY

We set up a fully three-dimensional realization of magnetic turbulence with wavevectors forming any angle with the background magnetic field $\boldsymbol{B}_0 = B_0 \hat{\boldsymbol{e}}_z$ and with a fine sampling of the Fourier space in order to avoid discretization problems (Pommois et al. 1998). The magnetic field is realized in a parallelepipedal simulation box (see Pommois et al. 1998, 1999), $\boldsymbol{B}(\boldsymbol{r}) = \boldsymbol{B}_0 + \delta\boldsymbol{B}(\boldsymbol{r})$, where $\delta\boldsymbol{B}(\boldsymbol{r})$ is the sum of static magnetic perturbations

$$\delta\boldsymbol{B}(\boldsymbol{r}) = \sum_{\boldsymbol{k},\sigma} \delta B(\boldsymbol{k}) \boldsymbol{e}^{(\sigma)}(\boldsymbol{k}) \exp i(\boldsymbol{k}\cdot\boldsymbol{r} + \phi_{\boldsymbol{k}}^{(\sigma)}), \qquad (1)$$

where $\phi_{\boldsymbol{k}}^{(\sigma)}$ are random phases and $\boldsymbol{e}^{(\sigma)}(\boldsymbol{k})$ are the two polarization unit vectors. Here we consider parameters relevant to the propagation of 1 MeV protons in the solar wind turbulence. For such particles, the velocity is $v \simeq 14{,}000$ km s^{-1}. Considering that the magnetic perturbations in the solar wind propagate with the Alfvén velocity $V_A \sim 40$ km s^{-1}, the assumption of static perturbations is well satisfied. Also, in the solar wind rest frame, we can neglect the electric field. The Fourier spectral shape is characterized by the turbulence correlation lengths l_x, l_y, and l_z and is given by

$$\delta B(\boldsymbol{k}) = \frac{C}{(k_x^2 l_x^2 + k_y^2 l_y^2 + k_z^2 l_z^2)^{\alpha/4+1/2}}, \qquad (2)$$

where we take the same spectral amplitude for both polarizations, and $\alpha = 5/3$ is close to the spectral index observed in the solar wind. Above, C is a normalization constant that is related to the level of fluctuations $\delta B/B_0 = [\langle \delta B^2(\boldsymbol{r})\rangle / B_0^2]^{1/2}$. In this model the turbulence anisotropy can be changed gradually from the isotropic case ($l_x = l_y = l_z$) to either the quasi–two-dimensional case ($l_x = l_y \ll l_z$) or the quasi-slab case ($l_x = l_y \gg l_z$), and nonaxisymmetric cases ($l_x \neq l_y$) may be treated as well. The constant-amplitude surfaces in Fourier space are ellipsoids, and the wavevectors are chosen as $\boldsymbol{k} = (2\pi/N_{\min})(n_x/l_x, n_y/l_y, n_z/l_z)$. The spectrum has cutoffs for both the short and the long wavelengths (band

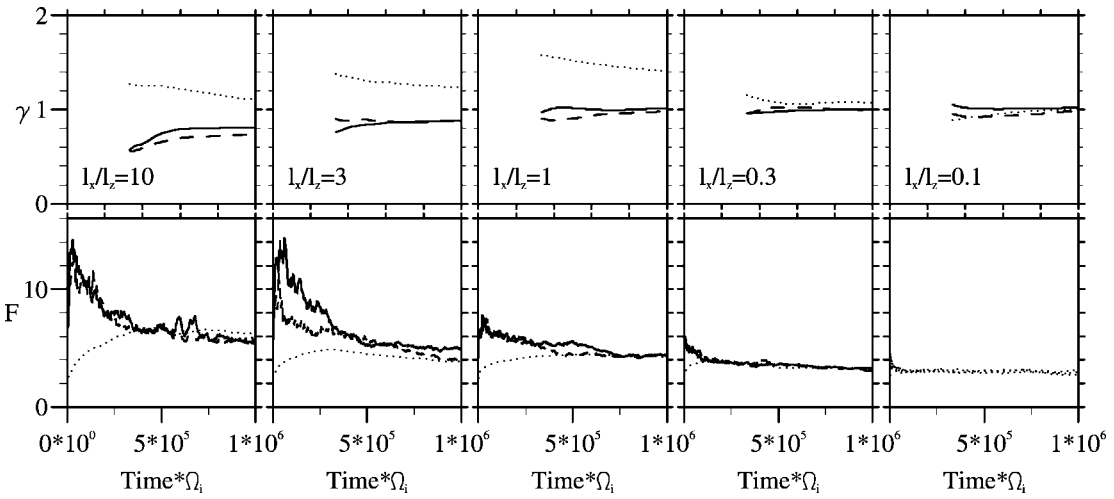

FIG. 1.—Anomalous transport exponents γ_i (*top panels*) and flatnesses F_i (*bottom panels*) are plotted as a function of time for $\delta B/B_0 = 0.5$, $\rho/\lambda = 3.2 \times 10^{-3}$, and $\rho/\lambda_{min} = 1.28 \times 10^{-2}$. Magnetic turbulence is axisymmetric, and the ratio of correlation lengths varies from $l_x/l_z = 10$ (*far left*) to 3, 1, 0.33, and 0.1 (*far right*). Results for the *x*-, *y*-, and *z*-directions are indicated by solid, dashed, and dotted lines, respectively.

spectrum) with $N_{min}^2 \le n_x^2 + n_y^2 + n_z^2 \le N_{max}^2$. In this way, the correlation lengths l_x, l_y, and l_z correspond to the largest wavelengths (in the respective directions) in the numerical model. For most of the runs presented here, $N_{min} \simeq 4$, and $N_{max} = 16$. The simulation box sides are given by $L_i = N_{min} l_i$ ($i = x, y, z$), so that at least four correlation lengths have to be traveled before the same magnetic configuration is found again. This effectively eliminates the periodicity effects (Pommois et al. 1998). We note that the need to have a fully three-dimensional spectrum leads to a shorter spectral extension than that found in the solar wind; the lack of short wavelengths may lead to an underestimate of wave-particle interactions, and especially of pitch-angle scattering, which depends on the gyroresonant interaction. To investigate the effects of the spectral extension, a few runs with $N_{max} = 32$ and $N_{max} = 48$ were also done.

In the solar wind, a turbulence correlation length λ is obtained from data in the radial direction. We assume that the radial correlation length λ is related to the turbulence correlation lengths of the numerical model by $\lambda^2 = l_z^2 \cos^2\psi + l_y^2 \sin^2\psi$ (Zimbardo et al. 2004), where l_z is along the spiral and l_y is in the plane formed by the average magnetic field and the solar wind speed. In the simulation, test particles are injected in the above magnetic configuration, and the trajectories are integrated with a high-precision fifth-order Runge-Kutta scheme with an adaptive step. Time is measured in units of the inverse of the proton gyrofrequency, $\Omega_i = eB_0/mc$. As typical values, we can assume $B_0 = 10$ nT and $\lambda \sim 0.03$ AU. For 1 MeV protons, this corresponds to $\rho/\lambda \simeq 3.2 \times 10^{-3}$. In order to determine quantitatively the transport properties, we compute the variances $\langle \Delta x_i^2 \rangle$, where $\Delta x_i = x_i - x_i^{(0)}$, as a function of time t. Then we make a fit of $\langle \Delta x_i^2 \rangle$ with the anomalous transport law $\langle \Delta x_i^2 \rangle = 2\kappa_i t^{\gamma_i}$ and determine γ_i and κ_i when t is large enough. The results presented here were obtained with $t = 10^6 \Omega_i^{-1}$; in physical units, this corresponds to more than 10 days for $B_0 = 10$ nT. Here the exponent γ_i characterizes the transport law: $\gamma_i = 1$ in the diffusive regime (Gaussian random walk); $\gamma_i < 1$ in the case of a subdiffusive regime; and $1 < \gamma_i < 2$ in the case of superdiffusive regime (Lévy random walk) (Klafter et al. 1987; Bouchaud & Georges 1990; Zaslavsky et al. 1993). In the case of Lévy random walk and of subdiffusion, the probability distribution function of particle positions can have long non-Gaussian tails. The importance of these tails can be measured by the flatnesses $F_i = \langle \Delta x_i^4 \rangle / \langle \Delta x_i^2 \rangle^2$, whose Gaussian value is 3.

Figure 1 shows the anomalous diffusion exponents γ_i, obtained by a running fit of the anomalous transport law, and the flatnesses F_i as a function of time, for $\rho/\lambda = 3.2 \times 10^{-3}$ and for $\delta B/B_0 = 0.5$, which is typical of the solar wind magnetic turbulence. The anisotropy is changed gradually from the quasi-slab case ($l_x = l_y = 10 l_z$) to the isotropic ($l_x = l_y = l_z$) and then to the quasi–two-dimensional case ($l_x = l_y = 0.1 l_z$). It can be seen that anomalous transport regimes, $\gamma_i \ne 1$, are obtained for the cases going from quasi-slab to isotropic; in particular, we find subdiffusion for transport perpendicular to $\boldsymbol{B}_0$, $\gamma_x, \gamma_y < 1$, and superdiffusion for transport parallel to $\boldsymbol{B}_0$, $\gamma_z > 1$. The non-Gaussian nature of these transport regimes is confirmed by the plots of the flatnesses, which show values much larger than 3 when transport is anomalous. On the other hand, for quasi–two-dimensional anisotropy, normal diffusion, $\gamma_i \simeq 1$, and Gaussian statistics, $F_i \simeq 3$, are obtained. Therefore, the results reported in Figure 1 show that the possibility of having anomalous, non-Gaussian transport sensitively depends on the turbulence anisotropy. We also performed simulations in the nonaxisymmetric case, $l_x > l_y \simeq l_z$, and the results are shown in Figure 2. By assuming the same fluctuation level ($\delta B/B_0 = 0.5$) and the same ρ/λ as for Figure 1, we can see that non-Gaussian regimes, i.e., superdiffusion along $\boldsymbol{B}_0$ and subdiffusion perpendicular to $\boldsymbol{B}_0$, are obtained as well. From both Figures 1 and 2 we can see that anomalous transport is obtained when $l_x \gtrsim 3 l_z$ (quasi-slab spectra), while normal diffusion in all directions is recovered for $l_x \lesssim 0.3 l_z$ (quasi–two-dimensional spectra).

Considering one of the cases for which parallel superdiffusion is found, $l_x/l_z = 3$, $l_y/l_z = 1$, and $\delta B/B_0 = 0.5$, reported in the right panels of Figure 2, we performed other runs by increasing the particle Larmor radius and varying the spectral extension. The left panels of Figure 3 report the simulation results for $\rho/\lambda = 1.02 \times 10^{-2}$ (corresponding to a proton energy of 10 MeV). It can be seen that γ_i is close to 1 for all of the *x*-, *y*-, *z*-directions. Also, the flatnesses reach, in the long time limit, the Gaussian value $F_i = 3$. In a similar way, nearly normal diffusion is obtained for the other two anisotropies in Figure 2 when the Larmor radius is increased to $\rho/\lambda =$

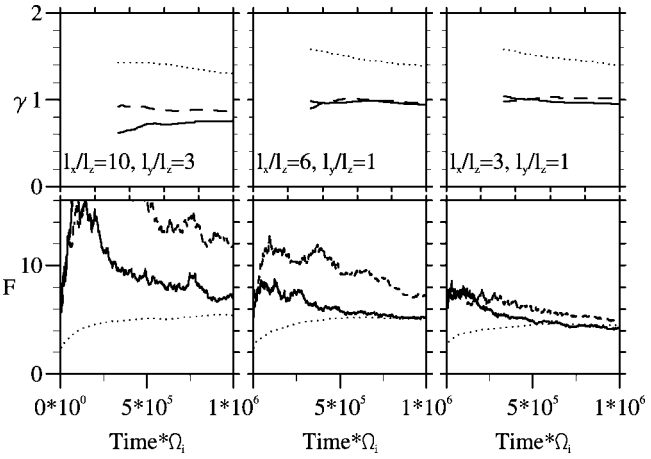

FIG. 2.—Same as Fig. 1, but for nonaxisymmetric anisotropy (as indicated in the panels).

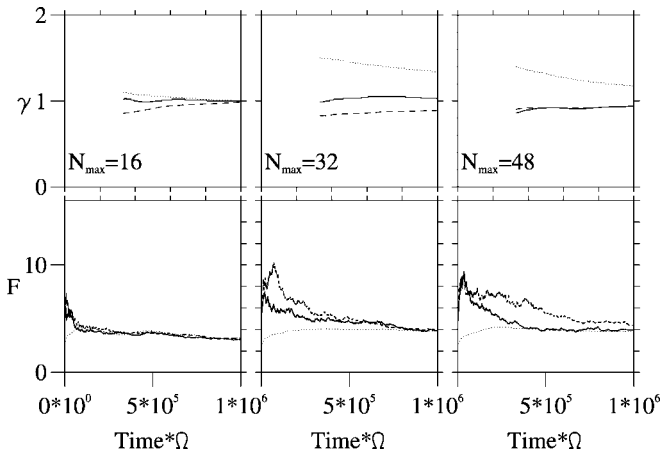

FIG. 3.—Same as Fig. 1, but for nonaxisymmetric anisotropy given by $l_x/l_z = 3$ and $l_y/l_z = 1$ and for different spectral extensions. *Left panels*: $\rho/\lambda = 1.02 \times 10^{-2}$ and $\rho/\lambda_{min} = 3.96 \times 10^{-2}$. *Middle panels*: $\rho/\lambda = 3.2 \times 10^{-3}$ and $\rho/\lambda_{min} = 2.56 \times 10^{-2}$. *Right panels*: $\rho/\lambda = 3.2 \times 10^{-3}$ and $\rho/\lambda_{min} = 3.84 \times 10^{-2}$.

1.02×10^{-2} (not shown). This means that by increasing the Larmor radius, ρ is closer to the shortest wavelength λ_{min} (for instance, for the run of the left panels of Figure 3, $\rho/\lambda_{min} = 3.96 \times 10^{-2}$, while for Figures 1 and 2, $\rho/\lambda_{min} = 1.28 \times 10^{-2}$), and wave-particle interactions are stronger. We performed two runs with a longer spectrum, by keeping $N_{min} = 4$ and by setting $N_{max} = 32$ and $N_{max} = 48$, respectively. These runs require very large numerical resources (P. Pommois et al. 2006, in preparation). Note that for $N_{max} = 48$, $\rho/\lambda_{min} = 3.84 \times 10^{-2}$, which is almost the same as for the left panels of Figure 3. The main result of these runs, shown in the middle and right panels of Figure 3, is that we still obtain superdiffusion along z, with $\gamma_z = 1.3$, 1.2, for $N_{max} = 32$, 48, respectively. This shows that superdiffusion is found with a longer spectrum, too, and that a small decrease in γ_z is obtained when λ_{min} decreases and becomes closer to ρ.

3. DISCUSSION

Considering the effects of the turbulence anisotropy for a fixed spectral extension, we have that when $l_x/l_z = 1$–10, parallel transport is superdiffusive (see Figs. 1 and 2). In these cases the particles, during gyromotion, are subjected to only weak variations of the magnetic field, so that pitch-angle diffusion is very slow (in other words, the magnetic moment is nearly conserved). Conversely, when $l_x/l_z = 0.1$–0.3, the transverse variation of the magnetic field is stronger, and the pitch-angle diffusion is faster, leading to a Gaussian diffusion process with $\gamma_z = 1$ and $F_z = 3$. Clearly, pitch-angle diffusion can occur also because of magnetic field variations along $\boldsymbol{B}_0$, due to the combined effect of parallel motion and gyromotion. Still, the present results show that pitch-angle diffusion due to $l_x < l_z$ is more effective than that due to $l_x > l_z$, as clearly shown by Figure 1. On the other hand, an increase in the Larmor radius allows particles to be subjected to stronger variations along their orbits, so that pitch-angle diffusion is increased. In the left panels of Figure 3 we have $\rho/\lambda_{min} = 3.96 \times 10^{-2}$ (large ρ, short spectrum), while for the right panels we have $\rho/\lambda_{min} = 3.84 \times 10^{-2}$ because of the longer spectrum. These two ratios are very similar, yet in the former case normal diffusion is obtained, while in the latter case parallel superdiffusion is obtained. Now, in the case of a limited spectral extension, the amplitude of the single turbulence modes, including those close to resonance with the Larmor radius, is larger than it would be in the solar wind. With a longer spectrum, the turbulence energy is distributed on a larger volume in $\boldsymbol{k}$-space, and the amplitude of the modes close to resonance is decreased. Since it is not presently possible to simulate a three-dimensional spectrum with an extension comparable to that of the solar wind, the possibility remains that we are underestimating pitch-angle diffusion because $\rho/\lambda_{min} < 1$. For instance, increasing the spectral extension γ_z goes from 1.4 to 1.3 and to 1.2, so that $\gamma_z = 1$ could be obtained with a realistic spectral extension. Still, the longer the spectrum, the smaller the amplitude of modes close to resonance, so that the actual value of γ_z in the solar wind remains open to further investigation. Therefore, we consider that parallel superdiffusion could be found for particles with small to moderate energies, which would resonate with small-amplitude modes of the spectrum.

If confirmed, the superdiffusive parallel propagation implies that there exist regimes where wave-particle interactions are present, but not so strong as to correspond to Gaussian statistics (Pommois et al. 2005); rather, the changes of parallel velocity correspond to a so-called Lévy random walk, in which the lengths of elementary displacements (scatter-free paths) have a power-law probability distribution (Klafter et al. 1987; Bouchaud & Georges 1990). An important, characterizing feature of Lévy statistics is that the second-order moment of the probability distribution of free path lengths is diverging. This means that the parallel mean free path $\lambda_\parallel$ can be, formally, infinite. This possibility can help us to understand why different values of $\lambda_\parallel$ can be inferred from the observations. In the case of parallel superdiffusion, the data have to be fitted with a transport law like $\langle \Delta z^2 \rangle = 2\kappa_z t^{\gamma_z}$, with $\gamma_z > 1$, so that two parameters have to be determined. Otherwise, the experimental determination of $\lambda_\parallel$ is very sensitive to the particular data set. We point out that recent studies of the magnetic flux tube structure in the solar wind indicate that an anisotropy with $l_x/l_z \simeq$ 3–10 can be appropriate for solar wind turbulence (Zimbardo et al. 2004), so that parallel superdiffusion could be the natural way of propagation of 1 MeV particles. Also, observations of SEPs that suggest scatter-free propagation may correspond to superdiffusion.

In the mechanism of diffusive shock acceleration, particles are accelerated by repeated crossings of the shock caused by diffusion due to turbulence. The acceleration efficiency depends in a critical way on the value of $\lambda_\parallel$ (Duffy et al. 1995; Ellison

et al. 1999). In the case of parallel superdiffusion, the acceleration rate will be decreased since the crossing of the shock is less frequent, especially at low energies where superdiffusion is more likely to happen. A diverging $\lambda_\parallel$ does not mean that particles are not crossing the shock again but that the acceleration rate has to be computed using totally new statistical tools, like the return probability for a Lévy random walk, rather than $\lambda_\parallel$. On the other hand, in the case of perpendicular shocks, the return of particles to the shock depends on perpendicular transport, and it is intriguing to notice that the perpendicular subdiffusion reported here may lead to an increased acceleration rate.

For perpendicular transport, we obtain subdiffusion for $l_x/l_z = 3$–10 (or larger) and normal diffusion for $l_x/l_z = 0.1$–1. Recent direct numerical simulations of particle transport in magnetic turbulence have shown that subdiffusive regimes can be found (Qin et al. 2002a) for perpendicular transport in the case of nearly purely one-dimensional (slab) turbulence. This process, called compound diffusion, is due to particles tracing backward the (magnetostatic) field lines. Qin et al. (2002b) were able to show that normal diffusion is recovered when a prevalence of fluctuations depending on the x- and y-coordinates (two-dimensional spectrum) is introduced. Here we can see that a moderately one-dimensional, or quasi-slab, turbulence also leads to subdiffusion, and we also obtain a quantitative assessment of the degree of anisotropy, $l_x/l_z \gtrsim 3$, needed to obtain compound subdiffusion. The concept of compound diffusion can be generalized by considering that, for the magnetic field lines, anomalous (superdiffusive or subdiffusive) transport transverse to $\boldsymbol{B}_0$ was obtained in cases of low stochasticity (Zimbardo & Veltri 1995; Pommois et al. 1998; Zimbardo et al. 2000). For small ρ/λ, perpendicular transport of particles could be looked at as the combined effect of transport along $\boldsymbol{B}_0$ and transverse field line transport. If we assume for particle parallel displacement that $z = [\langle(\Delta z)^2\rangle]^{1/2} = (2\kappa_z t^{\gamma_z})^{1/2}$, and for field line perpendicular transport that $\langle(\Delta x)^2\rangle = 2D_m z^{\alpha_x}$, we obtain a "generalized" expression of compound diffusion,

$$\langle(\Delta x)^2\rangle = 2D_m(2\kappa_z t^{\gamma_z})^{\alpha_x/2} \propto t^{\alpha_x\gamma_z/2}, \quad (3)$$

where we denote by α_x the anomalous transport exponent for magnetic field lines. A variety of values of $\gamma_x = \alpha_x\gamma_z/2$ can be obtained from equation (3) in the case of anomalous transport of either field lines and/or particles along z. However, inspection of the numerical results shows that equation (3) does not always apply, especially for $l_x/l_z < 1$. This fact can be explained by the exponential separation of field lines (Rechester & Rosenbluth 1978; Ruffolo et al. 2004; Zimbardo 2005) and by finite Larmor radius effects.

The perpendicular subdiffusion agrees with the finding of intermittent particle flux related to impulsive SEP events reported by the *Advanced Composition Explorer* (*ACE*; Mazur et al. 2000), since in such case particles remain confined in the coherent flux tubes present in the solar wind (Ruffolo et al. 2003; Zimbardo et al. 2004). On the other hand, the fast perpendicular propagation of SEPs in the heliosphere indicates that an efficient, possibly superdiffusive, perpendicular transport of particles is needed. Perpendicular superdiffusion, thanks to the nonlinear dependence of the mean square deviation on time, could explain both the small transport reported by *ACE* for short times and the fast propagation required by *Ulysses* measurements for later times (Zhang et al. 2003; McKibben 2005). A numerical exploration of the parameter space is under way in order clarify this issue.

This work was partially supported by the Italian INAF, ASI, and by the High Performance Computing Center of the University of Calabria (HPCC). P. P. acknowledges a grant from the AGROtrace consortium.

REFERENCES

Bieber, J. W., Matthaeus, W. H., & Smith, C. W. 1994, ApJ, 420, 294
Bieber, J. W., Wanner, W., & Matthaeus, W. H. 1996, J. Geophys. Res., 101, 2511
Bouchaud, J.-P., & Georges, A. 1990, Phys. Rep., 195, 127
Carbone, V., Malara, F., & Veltri, P. 1995 J. Geophys. Res., 100, 1763
Dalla, S., et al. 2003 Ann. Geophys., 21, 1367
Dobrowolny, M., Mangeney, A., & Veltri, P. 1980, A&A, 83, 26
Duffy, P., Kirk, J. G., Gallant, Y. A., & Dendy, R. O. 1995, A&A, 302, L21
Ellison, D. C., Jones, F. C., & Baring, M. G. 1999, ApJ, 512, 403
Giacalone, J., & Jokipii, J. R. 1999, ApJ, 520, 204
Jokipii, J. R. 1966, ApJ, 146, 480
Jokipii, J. R., & Parker, E. 1969, ApJ, 155, 777
Klafter, J., Blumen, A., & Shlesinger, M. F. 1987, Phys. Rev. A, 35, 3081
Kóta, J., & Jokipii, J. R. 2000, ApJ, 531, 1067
Matthaeus, W. H., Ghosh, S., Oughton, S., & Roberts, D. A. 1996, J. Geophys. Res., 101, 7619
Matthaeus, W. H., Qin, G., Bieber, J. W., & Zank, G. P. 2003, ApJ, 590, L53
Mazur, J. E., Mason, G. M., Dwyer, J. R., Giacalone, J., Jokipii, J. R., & Stone, E. C. 2000, ApJ, 532, L79
McKibben, R. B. 2005, Adv. Space Res., 35, 518
Pommois, P., Veltri, P., & Zimbardo, G. 1999, Phys. Rev. E, 59, 2244
Pommois, P., Zimbardo, G., & Veltri, P. 1998, Phys. Plasmas, 5, 1288
———. 2005, Adv. Space Res., 35, 647
Qin, G., Matthaeus, W. H., & Bieber, J. W. 2002a, Geophys. Res. Lett., 29, 1048
———. 2002b, ApJ, 578, L117
Reames, D. V. 1999, Space Sci. Rev., 90, 413
Rechester, A. B., & Rosenbluth, M. N. 1978, Phys. Rev. Lett., 40, 38
Ruffolo, D., Matthaeus, W. H., & Chuychai, P. 2003, ApJ, 597, L169
———. 2004, ApJ, 614, 420
Shalchi, A., Bieber, J. W., Matthaeus, W. H., & Qin, G. 2004, ApJ, 616, 617
Teufel, A., & Schlickeiser, R. 2002, A&A, 393, 703
Zaslavsky, G. M., Stevens, D., & Weitzner, H. 1993, Phys. Rev. E, 48, 1683
Zhang, M., McKibben, R. B., Lopate, C., Jokipii, J. R., Giacalone, J., Kallenrode, M.-B., & Rassoul, H. K. 2003, J. Geophys. Res., 108, 1154
Zimbardo, G. 2005, Plasma Phys. Controlled Fusion, 47, B755
Zimbardo, G., Pommois, P., & Veltri, P. 2004, J. Geophys. Res., 109, A02113
Zimbardo, G., & Veltri, P. 1995, Phys. Rev. E, 51, 1412
Zimbardo, G., Veltri, P., & Pommois, P. 2000, Phys. Rev. E, 61, 1940
Zurbuchen, T. H., Hefti, S., Fisk, A., Gloecker, G., & Schwadron, N. A. 2000, J. Geophys. Res., 105, 18327